Part II

INSTRUMENTS AND HARDWARE FOR THE BIOMAGNETIC RESEARCH

New scientific data are usually obtained with the improvement of the research technique. The case of the modern biomagnetism is a fine example of that. Even the titles of some publications underline that the corresponding area of research is related to the supersensitive magnetometry [9, 10].

As the book is meant primarily for specialists in the medical and biological field the authors have offered limited information about the technique of magnetometry.

An interested reader may find additional information on the subject in other publications [33, 35, 36, 39, 45, 69, 70].

Today, certain magnetometry techniques outlined here are not easily available. We hope, however, that soon magnetometry will become a routine method in the studies of biological objects.

Chapter 2

METHODS USED IN THE DETECTION OF THE MAGNETIC FIELDS OF BIOLOGICAL OBJECTS

Presently, the detection of MF of biological objects is performed with magnetometers varying in their design and structure. The first detection of MF from the human heart was performed with IM - a multiloop coil around a core of high magnetic permeability [46, 83]. IM can measure the MF component oriented along the sensor's axis. Notwithstanding certain

technical problems magnetometers of this type are still used in the magnetocardiographic research [108].

Since the early 70's some researchers abroad began to use SQUID - another type of magnetometer - in the measurement of MF of humans and animals [94, 148]. Like the IM, SQUID measures the MF component. Since SQUID is operated at temperature close to the absolute zero in the materials where resistance drops to the zero level the device's intrinsic noise is exceptionally low. It is highly unlikely that such a low intrinsic noise could be reached in magnetometry in the near future on the basis of a different physical phenomenon. Whatever is the case such low noise level may be assured only at low levels of magnetic interference.

In the late 70's there appeared publications on the use of the quantum optical pumping magnetometer (OPM) in the biomagnetic research capable of measuring the magnetic induction modulus [30]. Basically, OPM features spatial invariance and its readings are not related to the orientation. The OPM intrinsic noise in the frequency range below 50 Hz places OPMs between the IM and SQUID.

Apart from these there are other magnetometer types most effective in the measurement of relatively large magnitude MF of biological objects. Fluxgate magnetometer (FM) is an active coil IM model where extra power is fed to the coil for the core remagnetization. Theoretically, the FM intrinsic noise limit is controlled by the Barkhausen core ranging to the order of 1 pT in the frequency range abutting on zero. The actual noise threshold is one order of magnitude higher. Linear dimensions of the FM pick-up sensor are substantially smaller than of the IM used in registration of MF of the heart.

Magnetometers based on the Faraday effect (FEM) i.e. rotation of optical radiation polarization plane in optical fiber caused by magnetic field are in the development stage [103]. Sensitivity of FEMs is yet inferior to that of other magnetometer types. The relative simplicity and small dimensions of the FEM sensor constitute its main advantage. FEM basically measures the magnetic induction component.

The apparatus for noninvasive measurement of human cardiac cycle blood flow is another alternative used in the biomagnetic research. It is based on the blood magnetic susceptibility measurement [146]. The technique involves measurement of the MF of the studied object affected by an external MF. If the object is para- or diamagnetic the imposed MF causes it to magnetize proportionally to this field but with opposite polarity. Magnetization is effected along the MF direction in paramagnetics and reversely in diamagnetics. Similarly to water blood is diamagnetic. Its magnetic susceptibility is $0.7 \cdot 10^{-6}$.

SQUID with flux transformer (FT) has been used as magnetic signal probe in some experiments. The FT's signal loop is a differential circuit firmly fixed on the superconducting cylindrical magnet creating a 10^{-3} magnetizing field in the heart [146].

Another design of the hardware used to measure magnetic susceptibility features a different way of inducing an external MF involving a coil system and inducing a MF of varying magnitude [34,74].

Quite a number of publications are dedicated to designing hardware based on various effects for use in the biomagnetic research. Such literature may provide additional information on technical and methodological aspects of magnetic measurements [2, 5, 6, 14, 15, 25, 28, 41, 45, 47, 51, 75].

2.1. INDUCTION SENSOR

The first measurement of magnetic signal from the human heart was performed with induction sensors used in the differential detection circuit [83]. Operation of induction sensor is based on the electromagnetic induction caused in an electric circuit by variation of MF. Design of the sensor includes a multilayer coil around a core of high magnetic permeability.

The electromotive force (EMF) generated at the induction sensor is proportional to the MF variation rate over the pick-up coil. The EMF can be expressed as

$$E = - d/dt (\mu WSB \sin\alpha), \qquad (1)$$

where μ is effective magnetic permeability, *S* is coil loop square, *W* is number of coil windings, *B* is induction of the affecting MF, α is the angle between magnetic induction vector and coil loop plane.

The resulting EMF is a function of parameters μ, *S, B* and α variation over time. Whenever the parameters remain unchanged with the exception of *B* the transduction is classified as passive. It may be seen from formula (1) that a passive induction sensor is not sensitive to a permanent MF.

Sinusoidal variation of *B* will cause the resulting EMF change according to

$$e = W\mu S(dBx \sin \omega t/dt) = W\mu SBx \cos \omega t.$$

The wave form may be restored by integration, such as

$$u=\int W\mu SBx\cos \omega t = W\mu SBx \sin \omega t .$$

The product of $W\mu S$ is the transducer rate controlled exclusively by the transducer design characteristics. Effective permeability of the core is controlled by the proportion of its diameter to length, or to put it in other words, by the demagnetization rate *D*. Effective magnetic permeability μ may be estimated with regard to the demagnetization rate as follows

$$\mu = \mu r/[1+D(\mu r - 1)], \qquad (2)$$

where μr, is the initial magnetic permeability of the core material. For example, with $D = 0.1$ and $\mu r = 1000$ the maximal value of μ will not exceed 10. Shorter core length at the unchanged diameter will correspond to the lower transducer rate. As the transducer rate stability is related to the core stability it is also essential to accommodate variation of magnetic permeability caused by temperature, frequency and variation of MF, and permanent field magnitude. The IM owes its intrinsic noise to the thermal noise elicited by coil resistance *r* estimated as follows

$$em=(4kTr\Delta F)^{-1/2} \qquad (3)$$

where *k* is the Boizmann constant, *T* is temperature in Kelvin scale, ΔF is bandwidth. Spectral density of MF fluctuations equivalent to the thermal noise in the induction sensor accommodating the law that EMF

elicited in the coil is proportional to frequency, may be estimated as follows

$$SB=kT\,r^{-1/2}/\omega\mu WS. \quad (4)$$

Assuming that a sensor without a core has 10^4 loops of copper wire with total square S = 10^{-2} m^2 and r = 20 kOhm the spectral noise density at room temperature related to thermal noise in r will be 3 pT Hz$^{-1/2}$ at 10 Hz. Cooling down the sensor to the liquid helium temperature - 4.2 K will reduce the spectral noise density to 0.4 pT Hz$^{-1/2}$ at the same frequency. The induction sensor used in experimenting [83] had the spectral noise density of 5 pT Hz$^{-1/2}$ at 10 Hz. Induction sensor noise reduction may be achieved by introducing a ferrite core or any other high magnetic permeability material and concurrently reducing the number of windings to limit active resistance in the wire. This sensor was instrumental in detecting the alpha-rhythm MF of the human brain [92]. The potential of induction sensor with core is limited by the demagnetization factor. The problem of selecting the dimensions of a passive induction sensor to gain maximal sensitivity does not have a unique solution. A relatively large size of the sensor appears to be a disadvantage of IM used in the biomagnetic research as it reduces the precision of magnetic field source location. As regards noise immunity a point should be made to protect sensor from electrostatic fields and vibrations. Balancing the sensors used in the gradientometer circuit may be difficult. Low sensitivity of the induction sensor at low frequencies limits the ability to measure biomagnetic field. However, IM is more sensitive to signal over 1000 Hz than the modern superconducting magnetometers.

2.2. FLUXGATE MAGNETOMETERS

EMs are a variety of induction magnetometers with a high magnetic permeability core. The basic difference is that the core is located in the continuously remagnetizing MF i.e. parameter changes regularly. The FM output voltage is proportional to the MF applied along the core axis. The bandwidth ranges from zero to 100-1000 Hz [3, 4, 47].

Basically, the FM sensor consists of two cores made of high magnetic permeability material each with a copper wire winding. Cores with coils are positioned in parallel as close to each other as possible. Core windings, or else excitation windings, are counter connected and fed with the current from the excitation generator. A signal coil is wound around this core unit.

Alternating current excites an MF in the excitation windings severalfold larger in magnitude than magnetic saturation of the core. In the absence of external MF core remagnetization through the histeresis loop evokes pulses in the signal coil comprising a spectrum of excitation frequency components and odd harmonics. Counter connection of excitation coils markedly reduces penetration of a signal of the excitation frequency into the signal coil.

Whenever the external MF is evoked along the core axis the histeresis loop is shifted by magnitude of external field and voltage is induced in the signal core with the spectrum prevailed by the second harmonic of the excitation frequency proportional in its amplitude to the MF projection on the core axis. Polarity of the induced voltage alternates with the change of the external field polarity. The second harmonic signal is picked up by the narrow-band amplifier and transformed by the phase (synchronous) detector. Reference voltage at double frequency results from the excitation voltage. The phase detector output is connected to the third coil wound above the signal coil to establish the negative MF feedback which serves to expand the measurement range, and the FM bandwidth and to linearize the transfer characteristic.

Potential FM sensitivity is the function of the Barkhausen noise excited by the core domain walls motion created by the excitation field. The Barkhausen noise is also related to the quality of the core material. The equivalent spectral density of the noise remains more or less unchanged within the one to several hundred Hz range. The best commercial imported magnetometers have the noise level 10 $pT \cdot Hz^{-1/2}$. The best pilot FMs with circular core feature the spectral noise density of 0.3 $pT \cdot Hz^{-1/2}$ at frequencies over 3 Hz [75].

Fluxgate sensors are relatively small in size having:

diameter within I cm, and length within 2-3 to 5-8 cm. The circular core diameter does not exceed 2-3 cm. FM with circular core can be used in the biomagnetic research for detection of ion current in the body or inclusions in the human lungs. FM is quite sensitive to vibration and therefore has to be placed on a solid foundation. FM thermal drift is quite insignificant ranging from 0.05 to 0.1 nT/C°.

2.3. SUPERCONDUCTING QUANTUM INTERFERENCE DEVICE

SQUIDs are most commonly used in the biomagnetic research abroad. SQUIDs with a capability to detect MF from biological objects have recently developed in the USSR as well [7, 55]. SQUID employs the phenomenon of superconductivity of certain metals and alloys at low temperature (below 20K) and quantization of the magnetic flow through the superconducting material ring with low induction. Certain metals and alloys enter the state of superconductivity at the liquid helium temperature (4.2 K). In plumbum superconductivity arises at 7.18 K, niobium - at 9.2 K, vanadium - at 5.13 K, niobium-plumbum alloy - at 18.3 K [6, 26, 50].

Let us now consider the main phenomena occurring in superconductor in order to understand the physical nature of superconductivity and quantum interference A voltmeter connected to the input and output of direct current through a metal in a state of superconductivity will show no voltage drop in the metal. Should the superconducting material be divided into two parts the current will cease and voltmeter will show the voltage identical to the one in a disconnected circuit of power supply.

Reduction of the gap between the two parts of the superconductor to 1-2 nm may trigger an interesting phenomenon involving the absence of voltage and presence of direct current between the two parts of the superconductor. Under these circumstances current goes via a narrow gap. This phenomena is called dc Josephson effect. There is another ac

Josephson effect when an electric current flows through the superconductor with the voltmeter showing certain voltage while electromagnetic energy is emitted from the gap in the superconductor [28].

The both effects are due to the unique state of superconductivity. We are more concerned with the dc Josephson effect as it is used in the highly sensitive magnetometers.

A common metal resists electric current because any directed flow of electrons gives rise to energy loss due to dispersion of individual electrons by oscillation of atoms or by admixtures in the metal and lattice defects. However, whenever motion of each electron is correlated in phase with the others and this correlation affects the entire metal, dispersion of one electron will inevitably cause all others to disperse.

Dispersion of electrons is highly unlikely under the state of superconductivity. Having emerged the superconducting current becomes immune to dispersion accounting for resistance to the regular current.

This reasoning was the first step to find the explanation for the superconducting current. Subsequently, it was specified that the current was not a collective motion of individual electrons but rather of electron pairs. As is known electrons tend to repulse one another in a free space. However, interaction among them in the metal is different. Traveling through the metal ion lattice an electron with a negative charge attracts positive ions and deforms the lattice. It creates the excessive positive charge in the trace of an electron which may attract another electron. Therefore, it appears that apart from the common repulsive force affecting electrons there emerges an indirect attraction evoked by the lattice of positive metal ions. The metal becomes superconducting when the force of attraction elicited by the lattice exceeds the repulsive force and the summary interaction among electrons operates as the force of attraction.

This approach, perhaps, explains why certain high-conducting metals such as silver and copper are not superconductors. The weaker interaction between electrons and the lattice in the high-conductive metals reduces attraction of electrons elicited by the lattice which is believed to

cause the superconductivity. Accordingly, the current in superconductor is evoked not by the motion of single electrons as it happens in regular circumstances but rather by pairs of electrons. As the linkage between electrons is quite weak it is easily broken whenever superconductivity discontinues.

The average distance between the two coupled electrons in the state of superconductivity is thousands times more than between the ions in the metal lattice. As there are several electrons for every ion the electrons of each coupled pair are positioned in the volume containing millions of pairs. It stems from the quantum mechanics that the motion of all the electron pairs in this case is 100% correlated.

An electron pair may be presented as wave with wave length $\lambda = P/h$, where P is the mass center impulse, h is the Planck's constant, relying on the wave characteristics of electron. According to the quantum-mechanical wave pattern equal mass center impulses of all pairs imply that waves corresponding to the pairs have equal lengths. Apart from having identical length the waves of all pairs in the superconductor are in the same phase. Phase identity of all pairs in the superconductor is a quantum-mechanical effect on the macroscopic level.

Pair phases should be identical along one superconductor length because pairs can freely move in it. If the superconductor is broken, pairs cannot interchange. However, if the gap is narrowed, a certain intermediate position may be created when some exchange of pairs takes place owing to the quantum-mechanical process otherwise known as tunnelling. Due to their wave nature electrons may tunnel or penetrate through a barrier which they could not make if they were simple particles. Tunnelling of pairs between the two parts of the superconductor creates an in-phase relationship at the superconductor ends. It can be changed with electric or magnetic field [6, 28].

Let us consider a ring-type SQUID with one tunnel junction housing a superconducting current. The electron pairs in the SQUID must be in phase to sustain superconductivity i.e. in the process of circling the ring

their phase must change by a whole number of the phase period of 2π radian. This can be mathematically represented as

$$2\,n\pi = \Theta + 2\pi\Phi/\Phi o,$$

where Φo is the quantum of magnetic flow of $2.07 \cdot 10^{-15}$Wb.

The second term in the right part of the equation determines the phase shift caused by the magnetic flow Φ through the SQUID ring. As the flow increases the flow in the ring increases stepwise by one quantum of the magnetic frow Φ. Each step-like increase changes the phase by the magnitude close to Φo. Its change is correlated to increase in the external field pointing out to the periodic relation of the phase difference at the junction featuring period $\Delta B = \Phi/S$, where S is the area of the SQUID ring. It is interesting that the period does not depend on the SQUID type.

In a superconducting ring with two dc Josephson junctions the current interference occurs in the ring if the operative dc reading i fed to the ring from an external source is slightly higher than the critical current ic creating the difference of potentials u at the SQUID.

The current evoked in the SQUID affects the two junctions differently. It is added to the operative current in one junction and subtracted in another. In result the current in the ring with two junctions is periodically related to the external MF through the ring. The current maximum occurs at $\Phi ext = 0, \Phi o, 2\Phi o...$ and the minimum $\Phi ext = \Phi/2, 3\Phi o/2...$. The process makes the voltage at SQUID change periodically. The alternation amplitude may reach approximately 10 mcV.

Direct voltage measurement in the one-junction SQUID design is not feasible because the connecting wires are short-circuited to the superconducting part of the ring. Therefore, the external MF impact on SQUID can be measured at rf.

Topologically, rf SQUID is a superconducting ring with weak link which holds down the current evoked in the ring by the given external flow and eventually interferes with the regular flow quantization. Besides, the weak link con trols the critical current in the ring i.e. the maximal

magnitude of the current in the ring causing no voltage drop in it. The SQUID link is regulated to assure that whenever the current reaches the critical magnitude and the weak link leaves the superconducting state back into normal

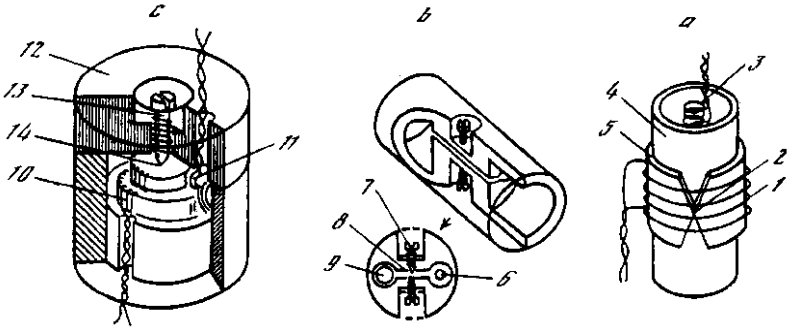

Fig. 2. Types of rf SQUID
a - thin film cylindrical: 1 - input coil, 2 - weak link, 3 - rf coil, 4 - nonconducting body, 5 - thin superconducting film; *b* - two-junction SQUID; 6 - rf coil, 7 - sharpened screw, 8 - weak link, 9 - input coil; *c* - toroidal: 10 - input coil, 11 - rf coil, 12 - niobium body, 13 - sharpened screw, 14 - junction

for a short while, the current in the ring should change merely by one quantum. Following this, the weak link regains its superconducting state because the compensation current in the ring drops below the critical level.

The modern SQUID "ring" is a massive niobium unit; its weak link is a tunnel junction formed by an isolating oxide barrier or a point contact between the sharpened end of the niobium screw and the niobium unit. Three SQUID types are most commonly used to perform biomagnetic measurements. They are the thin-film, two-junction and torroid SQUIDs (Fig. 2,*c*). Each device has a superconducting input coil as a part of the flux transformer and a copper rf coil performing the SQUID control function.

As regards the two-junction dc SQUIDs they are manufactured on the basis of the thin film circuit technology. They have already been employed in the biomagnetic measurements.

The electric circuit of the one-junction rf SQUID is presented at Fig. 3. The rf displacement field is evoked by the current from the rf generator through the rf coil with induction $L1$ coupled with the SQUID. Induction $L1$ and capacitor $C1$ together make an oscillatory circuit.

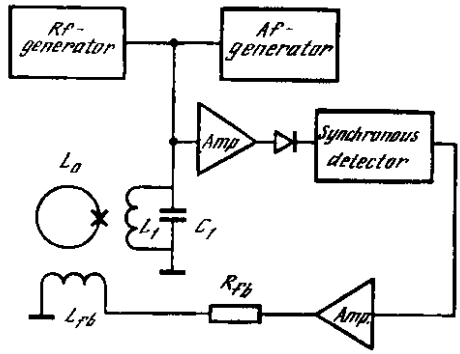

Fig. 3. Electric circuit of a one-junction rf SQUID. (Explanation in the text)

Usually, it is tuned to about 20MHz. Its oscillation starts with the resonance frequency from the rf generator. The current evoked by generator *Ir* is considerably smaller than the current *Ik* in the rf circuit. Their relation may be expressed as $Ir = Ik/ Qc$ where *Qc* is the circuit reliabiliity. If the *Ik* current amplitude is high the SQUID passes through the two full histeresis loops during the period of the current. At one loop a quantum of magnetic flow is taken in, and it is taken out at another. Energy losses in the SQUID junction losing the state of superconductivity for a short while are represented by variation of the oscillatory circuit's total resistance and the related voltage variation in it.

The circuit also involves a modulated signal generator and synchronous detector operated as the feedback circuit. This design works to expand the measurement range. The circuit is sometimes referred to as the magnetic flow lock because the magnetic flow averaged at the rf signal period through the SQUID ring is maintained invariable i.e. SQUID operates as a null-detector. The feedback current is fed to the coil *Lfb*. In result the

feedback resistance *Rfb* causes the voltage drop proportional to the measured magnetic flow. The modulating field *fm*, variating in the square-wave pattern is evoked at the 100 kHz frequency which assures uniform frequency response from zero to the upper limit frequency of *fm*/2 Amplification and the time constant of the feedback circuit limit the maximal velocity of the magnetic flow variation. A regular maximal tracking velocity of a commercial SQUID is about 10^7 Φo/s.

The basic sources of noise in the rf SQUIDs are the first amplification stage, rf circuit elements at the room temperature and the SQUID intrinsic noise. The latter is caused by fluctuation of the current in the SQUID ring at the thermodynamic equilibrium when the rf field brings the current to the critical level. The rms of the magnetic flow vs magnetic noise variation in commercial devices may be expressed as

$$S\Phi^{1/2} = 10^{-5}\ \Phi o/Hz^{1/2}$$

The SQUID general sensitivity may be shown as the minimal energy of signal fed to the coupling coil generating the output voltage equal to the rms noise level in the 1 Hz band. The energy sensitivity is measured in joule-s or joule/Hz. Common energy sensitivity of commercially manufactured devices is $2\cdot10^{-28}$ J/Hz. Experimentation with SQUIDs has indicated that the energy sensitivity may reach $7\cdot10^{-31}$ J/Hz and the quantum limit may be within $1.1\cdot10^{-34}$ J/Hz [45].

As a rule the SQUID noise spectrum remains uniform to a certain low frequency. However, at still lower frequencies the noise appears to grow. Although the source of that noise is the SQUID its mechanism has not yet been understood.

SQUID is essentially the device to measure the external MF flow through the SQUID ring area. Its resolution cannot be improved by a simple increase of its area because its induction *Lo* is limited. For one thing, if the thermal fluctuations with energy ~ *kT* (*T* is temperature of 4.2 K; *k* is the Boltzmann's constant) are not to interfere with the Josephson effect in the weak link it

requires that $Lo < \Phi o^2/kT$ [50]. For another, the increase of *Lo* corresponds to reduction of the critical current *icr* through the Josephson junction related to *Lo* through $Loicr \sim \Phi o$ implying that reduction of the critical current corresponds to lesser stability of the junction action. As a rule,

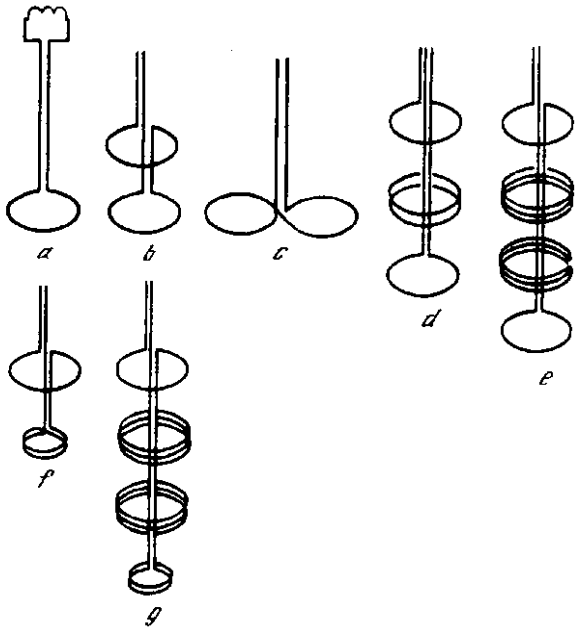

Fig. 4. Types of magnetic flux transformers. (Explanation in the text)

the SQUID ring area is about several square mm. An increased number of SQUID loops allows to expand it to several dozens sq.mm.

SQUID with a small size ring may be used with a device designed to dramatically expand the pick-up area i.e. magnetic flux transformer (FT) (Fig. 4, *a*). FT is a closed loop made of superconducting material wound in two places of the coil. Signal coil with induction *Ls* should be placed in the SQUID opening to assure maximal coupling effect and the pick-up coil with induction *Lp* is placed in the measured MF.

As FT is a closed superconducting loop its magnetic flux remains unchanged i.e. variation of MF in the *Lp* loop evokes a superconducting

current preventing variation of the summary flux in the loop. The evoked current in the signal coil *Ls* elicits a flux in the SQUID which can be measured. Optimal flux transfer into the SQUID occurs if *Ls* = *Lp*. FT serves to dramatically expand the SQUID's effective area. However, it appears to be limited by the fact that its increase gives rise to the *Ls* increase and coupling coefficient between the pick-up coil and the SQUID drops. At the same time large pick-up coil is unreasonable in the biomagnetic research because it holds the risk of reducing the coupling coefficient between the signal source and the pick-up coil. The optimal pick-up coil size in SQUIDs with FT is about 1 to 3 cm. A pick-up coil consisting of two windings with equal area wound counter- and clockwise and separated by a certain (base) distance will measure the difference of the MF flux in points occupied by the windings (Fig. 4, *b*). Whenever the magnitude of the flux difference is smaller than the flux we may speak of the gradient variation and the device is operated as a gradientometer. (The term "gradiometer" is preferred in publications abroad).

It is the common characteristic of all pick-up coils that the sum of products of the loop number by the area at all sections of the coil equals to zero. The loops taking the current clockwise are referred to as positive, and the ones with the counterclockwise current as negative. In case of a symmetrical second-derivative gradiometer (Fig. 4*d*) the coil would consist of three sections with the loop ratio I:-2:1. In the third-derivative gradiometer (Fig. 4,*e*) the coil would consist of four sections with the loop ratio I : -3 : +3 :-1. The spatial selection zone may be reduced by using asymmetrical (Fig. 4, *f, g*) coils with the total loop area equal to the area of one loop.

Linear position of the pick-up coil axes in the gradiometer (Fig. 4*b*) will make it measure the ∂Bz/∂Z gradient component. However, their planar position (Fig. 4, *c*) will make it measure the ∂*Bx*/∂*Z* gradient component.

Areas of the pick-up coils must be identical to assure maximally reduced MF from sources of interference. Their identity is accomplished

by fine tuning devices made of small pieces of the superconducting material. Moving them between the pick-up coils it is possible to equalize their effective area because the superconductor works to throw away the MF and thus to reduce the operative pick-up area. Such

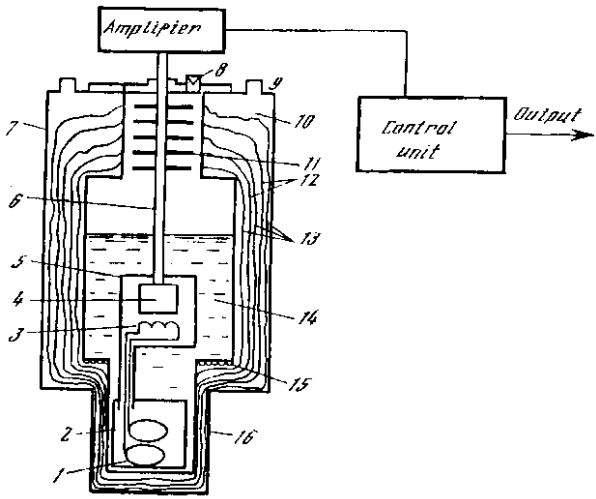

Fig. 5. First-order rf SQUID gradiometer. (Explanation in the text)

a mechanism can perform equalization in the order of 10^{-5}-10^{-6}.

It has been reported recently that the rf circuit may be coupled to several SQUIDs simultaneously [45]. In that case each SQUID must have its own FT and the pick-up coil. Modulation would be performed not through the circuit's coil but rather through the FT circuit. Each SQUID would operate on its own modulated frequency to be later divided by synchronous amplifiers. The advantage of this design is seen in the possibility to build a device for the simultaneous measurement of three orthogonal MF components and the MF gradients.

One of the publications [85] describes a gradiometer performing

measurements in three spatially distributed points. This type of a gradiometer is quite handy to identify spatial zones of the evoked MF of the brain.

A seven-channel SQUID magnetometer for brain research is a new development in the field of multichannel SQUIDs [106]. It is distinguished by channel divided by the pumping frequency allowing to dramatically reduce the mutual noise level with the use of the special type FT. Such a multichannel SQUID is a magnetometric system which can be operated only in a shielded chamber.

Building multichannel gradiometers capable of supplying data on the spatial MF from a biological object is the general development trend of the magnetometric hardware used in the biomagnetic research. Multichannel gradiometer appears to be an indispensable instrument for the spatial localization of MF sources in the human cortex and heart responsible for various electromagnetic processes. This research is also impeded by certain technical problems such as elimination of the mutual magnetic impact of the neighboring FTs in SQUIDs and their electric circuits.

Let us consider a typical design of the first-order rf SQUID gradiometer presented in Fig. 5. The SQUID system consists of: 1 - gradientometric type pick-up coil, 2 - high frequency screen, 3 - SQUID coupling coil, 4 - SQUID, 5 - superconducting screen, 6 - SQUID output, 7 - helium dewar, 8 - helium vapor outlet, 9 - pump connection, 10 - vacuum shell, II - shields (radiation screens), 12 - steel bands cooled by helium vapor, 13 - superinsulator, 14 - liquid helium, 15 - molecular mesh to stop infiltrated helium vapor, 16 - dewar tail.

The SQUID's pick-up coil is placed usually as close to the dewar's bottom as possible where the studied object is supposed to be. As a rule, the preamplifier is positioned on the dewar's cover and connected to the control unit, amplifier and signal detector by a cable system. The dewar's design allows its vertical inclination to 40-45° depending on the liquid helium level.

It is important for the user that the SQUID's output signal looks quite different from outputs of other electronic devices. As each response cycle is identical to other cycles it is not possible to estimate the absolute

magnitude of the MF induction component. What can be done is to estimate merely its increment by the number of cycles with electronic counter or by stabilizing the full SQUID field electronically. The second technique is more popular in the biomagnetic research as it assures the broadest measurement range.

The other feature of the periodic response is represented in the fact that at the impact of interference from vibration, radio stations, radar stations, electrostatic discharge and many other sources the SQUID system may lose its stability at an individual response peak and disrupt it entirely. For this it is sufficient to have the noise level of the order of O.I nT. Such a low noise resistance of SQUID makes it imperative to carefully follow the assembly procedure and to use screening, but, of course, not against the frequencies measured by SQUID.

In the late 1986 Muller and Bednorz discovered the high temperature superconductivity observed in the lanthanum-barium-copper-oxygen ceramics at temperatures above 30 K. By the early 1987 some countries, the USSR included, have manufactured high-temperature superconducting materials with operational temperature of the order of 100 K being higher than the liquid nitrogen temperature (77 K).

All this has nourished the hope that there will be soon created liquid nitrogen magnetometers and gradiometers using the Josephson effect. Apparently, their sensitivity will be several times inferior to that of the similar devices operating on the liquid helium. Therefore, in is anticipated that the liquid helium magnetometric hardware will remain as important to the neuromagnetic research in the near future.

It is felt that the high temperature superconductivity in future could be employed in making screens to suppress the external noise.

2.4. OPTICAL PUMPING MAGNETOMETERS

OPM has been developed to perform precision measurement of MF at the Earth's surface and orbits of man-made satellites. It has been reported [30] that it can be also used in the biomagnetic research - magnetocardiography, magne-topneumography (study of hazardous magnetic inclusions in the lungs) and evaluation of the excess iron content in

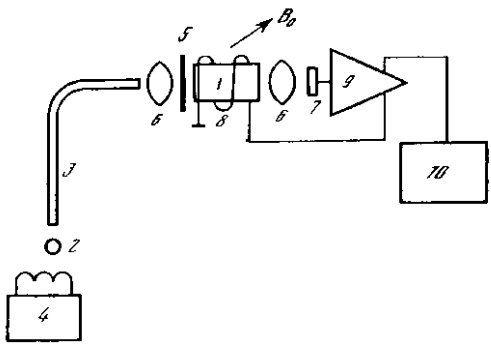

Fig. 6. Optical pumping magnetometer. (Explanation in the text)

the liver, etc.

The OPM is based on the optical resonance orientation of the paramagnetic atoms and the magnetic resonance [40, 88].

OPM consists of (Fig. 6): 1 - absorbing cell with the paramagnetic substance vapor, 2 - spectral lamp, 3 -light guide, 4 - spectral lamp high frequency exciter, 5 - circular polarizer, 6 - lenses, 7 - photosensor, 8 - rf coil, 9 - wide-band amplifier, 10 - frequency measuring unit.

The light emitted by the spectral lamp is led to absorbing cells through 75 cm long light guides. This length is required to withdraw spectral lamp exciter with its ferromagnetic elements (transistors) away from the sensitive elements and to eliminate electromagnetic deviation evoked by the feed current supplied to the exciter.

The spherically shaped spectral lamp has a diameter of about 10 mm. It contains an alkali substance and buffer gas to facilitate triggering of the high frequency discharge. The circular polarizer is made of an infra-red polaroid and a quarter wave plate. Their optical axes are positioned at 45° to each other. The absorbing cell is a cylinder with optically polished plates. An alkali metal is inserted into the cell via a side outlet under vacuum. Inner walls are covered with a thin paraffin layer to improve the cell quality.

Cesium - the most easily available alkali metal having only one stable isotope (^{133}Cs) is widely used in the OPM. The spectral lamp and the absorbing cell contain vapor of the same substance. Isotopes of other alkali metals such as rubidium, potassium and gaseous helium can also be used as the working substance.

The working substance controls the absorbing cell temperature allowing to obtain the maximal signal magnitude. Operated on cesium the OPM coil may be used within the room temperature range i.e. 17-30° C.

In order to understand the principle of optical pumping one should proceed from the assumption that alkali metal atoms have the energy structure allowing its ground state to split at the impact of the external MF into two sublevels corresponding to the atomic spins orientation along and counter the MF direction. The number of -1/2 and +1/2 atomic spins in the Earth's or similar MF is approximately the same. The excited state of atom P may be represented at one level (Fig. 7). This hypothesized structure clearly shows the role of optical radiation.

In the absence of the circular polarizer the optical radiation from the spectral lamp goes through the absorbing cell containing cesium vapor and is partially attenuated due to absorption in the vapor. Absorption of light in the cell is caused by atom's transition from the ground state S into the excited state P with the subsequent spontaneous transition back to the ground state. The excited state duration is about 10^{-8}s. There is an equal number of atomic spins oriented along the MF *Bo* direction and counter it i.e. the energy state

of atoms does not change under the nonpolarized radiation impact.

A circular polarizer placed before the absorbing cell qualitatively changes the absorption process and atom's distribution to sublevels of the ground state. The circularly polarized optical resonance radiation is

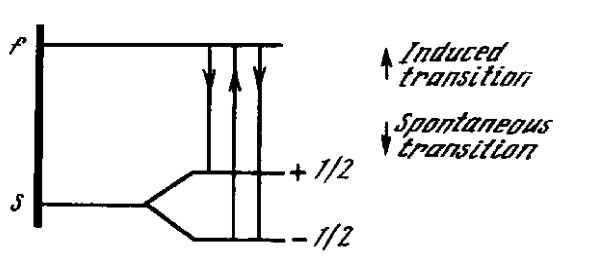

Fig. 7. The energy structure and transitions of the hypothetic alkali metal atom. Splitting of the state is the function of the external MF induction

described by a certain angular momentum accounting for different interaction between the light and the atoms at the +1/2 and -1/2 sublevels. In case of the right-hand light polarization atoms have a better chance of transition to the higher excited level from the -1/2 level than from +1/2. However, the chances of spontaneous transition from the level P to the sublevels of the ground state are equal. Therefore, we deal with a mechanism causing devastation of the -1/2 level in the course of time and occupation of the +1/2 level.

As soon as the process reaches in a certain time its nonequilibrium stationary state the quantity of the light passing through the cell would increase as against the initial conditions. In other words the cell would become more transparent.

Velocity of reaching the nonequilibrium stationary state ($1/\tau 1$) is the function of the optical pumping ($1/Tp$) and collapse ($1/T1$) velocities:

$$i/\tau 1 = i/Tp + 1/T1,$$

where Tp is the time of optical pumping, $T1$ is the time of longitudinal relaxation.

Collisions of atoms among themselves and with the container walls cause the nonequilibrium stationary state to collapse. The alternating current with ωo frequency fed to the rf coil wound around the absorbing cell, meeting the ωo = γ*Bo* requirement, where y is the gyromagnetic atomic ratio and *Bo* is the external field induction, will cause the alternating magnetic field to break the light-evoked nonequilibrium state. In other words, quantities of atoms with +1/2 and -1/2 spins at the ground state sublevels will be equalized. This effect is referred to as magnetic resonance. The precise magnitude of the atomic constant y measured in rad/ T s is exactly known.

The continuously destroying action of the resonance rf field will cause the quantity of the light getting to the photosensor to reduce since the light absorption required to reach the nonequilibrium stationary state will increase. If frequency $\omega \neq \omega o$, the rf field will not cause the quantity of the light passing through the absorbing cell to change. Apart from changing intensity of the passing light at the time of the resonance rf field action, the optical radiation is modulated with rf field frequency if the angle between the induction B vector and the optical axis is not 0 or 90°. As a rule the extent of the light modulation is not big and makes 0.1-1% of the exposure level.

The width of the magnetic resonance line is estimated as

$$\Delta\omega = 1/\tau 2,$$

where τ2 is the time of the transverse relaxation describing the impact of the atoms collision with the absorbing cell walls. In the case of the absorbing cells without the buffer gas but with internal walls coated with saturated hydrocarbons (paraffins) to increase the time of relaxation τ1 should be 3-7 fold more than τ2.

The OPM sensor is essentially a transducer of the modulus of MF induction vector into frequency or phase variation depending on the resonance rf field introduction mode. The effect of the resonance frequency MF on the polarized ensemble of atoms elicits a photosensor output signal at the same resonance frequency. Then, the signal phase within

the resonance line width may be estimated with

$$\varphi = \pm \pi/2 \pm \text{arctg}\, \Delta\omega\tau,$$

where $\Delta\omega$ is tuning out relatively the resonance frequency $\Delta\omega o$ assuming that phase shifts in the photosensor and amplifier are close to zero.

Given the permanent resonance frequency and the variating MF within the resonance line the phase difference between signals at the rf coil input and the amplifier output represents the measure of the magnetic field:

$$\varphi = \pm \pi/2 \pm \text{arctg}\, \gamma B \tau 2.$$

If the amplifier is locked on the rf coil through a device performing the $\pm\pi/2$ phase shift at the resonance frequency this will meet the phase balance requirement of self-oscillation. The phase balance is established if the sum of phase shifts in the feedback loop equals zero. The other self-oscillation requirement is the amplitude balance i.e. the feedback loop transfer rate of 1:1 or higher, which can be easily met.

The photosensor loaded to maintain its phase shifts φ = -arctg *R1Ctr* close to $\pi/2$, where *R1* is the load resistance and *Ctr* is the transition capacity of the semiconducting photosensitive diode, is often used as a phase-shifting circuit.

In other cases the photosensitive diode is short circuited and *R1* corresponds to a very low phase shift. In order to meet the $\varphi = \pm \pi/2$ requirement the amplifier is complemented with a separate phase-shifting circuit such as an integrator where φ is equal to $\pi/2$ within a certain frequency range.

In order to limit the self-generated oscillations amplitude the amplifier may be also complemented with the automatic gain control (AGC) or the amplitude limiter.

The OPM coil self-oscillation circuit is essentially the frequency transducer of the module of MF induction vector. The coil is actually capable of accurately following MF variations within the frequency range (MF induction) meeting the phase and amplitude balance requirement.

The OPM coil sensitivity is related to the photon shot noise, dark current of the photosensitive diode and the noise emitted by the amplifier's first stage. The second and third sources make a considerably lower contribution into the total noise level. It has been established experimentally that

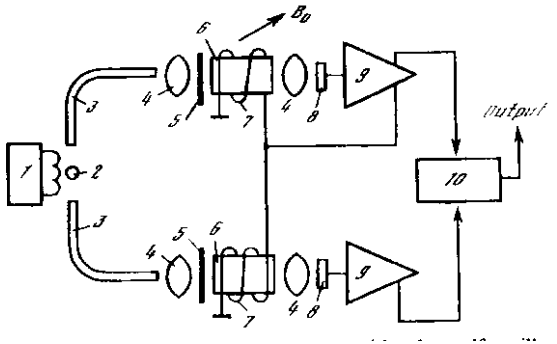

Fig. 8. The first-order OPM gradiometer with the self-oscillation and filter type coils
I - spectrometer lamp exciter; 2 - spectrometer lamp; 3 - light guides; 4 - lenses; 5 - circular polarizers; 6 - absorbing cells with the working substance vapor; 7 - rf coil; 8 - photosensors; 9 - amplifiers; 10 - phase meter

the coil spectral noise density is 200 - 400 ft/Hz$^{-1/2}$ within the 0.5 - 30-35Hz. According to the theoretical estimate the OPM potential sensitivity is around 10 fT in the I Hz band [2].

The first order gradiometer is built with a self-oscillation and open feedback sensors. Its block-scheme is presented in Fig. 8. The device is designed to measure phase difference between the input and output signals of the coil with the open feedback loop. The impact of the local MF on the open loop sensor causes the phase difference to vary in proportion to the operative local MF. The impact produced on the self-oscillation sensor causes its oscillation frequency to alter and the frequency alternation into the phase change due to the open loop sensor [16].

The disadvantage of the gradiometer with two different type coils is that their frequency characteristics and response to the MF variations are

different. This does not provide maximum possible suppression of the magnetic noise evoked by large amplitudes. The disadvantage may be neutralized in a gradiometer using three sensors: two with the open loop and one of the self-oscillation type to support the first two.

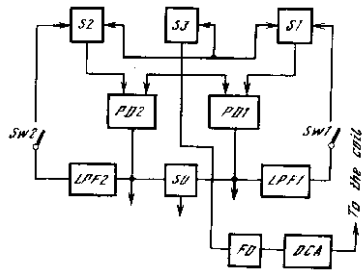

Fig. 9. The block-scheme of the second-derivative OPM gradiometer with active noise reduction. (Explanation in the text)

Gradient may be measured between any pair of sensors. However, the pair of the open feedback loop sensors will feature the best noise resistance [37].

Depending on the assignment the gradiometer's sensors may be positioned at different spatial locations such as in a line or at the corners of an equilateral triangle. Positioning of sensors in the corners of an equilateral triangle makes it possible to perform simultaneous measurement of two MF gradients of the human heart tantamount to taking measurement from two leads. Positioning of three sensors in line gives us a second-derivative gradiometer. The block-scheme of the second-derivative gradiometer in Fig. 9 shows an extra unit used to perform subtraction of the one gradiometer measurement from another in order to increase the spatial noise resistance of the measurements.

Operation of the second-order gradiometer both with OPM and SQUID sensors requires balancing of the coil pairs. Quality of balancing is represented by an arbitrary unit showing the external uniform field reading reduction versus the field itself. Assuming that in a uniform MF the

gradiometer shows instead of zero a certain specific reading equivalent to a certain gradient ΔBo, the quality of the balancing will be represented as $\Delta Bo/Bo$. In the second-order OPM gradiometers it is estimated as a value of the order of 10^{-7} -10^{-8}.

The minimal base distance is defined by the geometrical dimensions of the absorbing cell. It might be 5-5.5 cm in a 80 cm^3 absorbing cell.

Bandwidth of gradiometer depends on the half-width of the magnetic resonance line which is the function of the pumping light intensity. As a rule it is set to have the 30-40 Hz bandwidth at 0.7 level.

To measure the spatial distribution of MF from a biological object with a one- or two-channel gradiometer it is necessary to move from the one point in space to another by shifting either the object or the sensor. The procedure may take a relatively much time - to the order of dozen seconds or even several minutes for a full cycle involving many measurement points. Over this time parameters of the MF source in the object may alter due to certain physiological or psychological causes. Under these circumstances it will be necessary to use multichannel gradiometers to obtain a one-time spatial picture of the MF distribution.

Building an OPM multichannel gradiometer is easier because its sensors operate at a single resonance frequency with minimal mutual interference. The scheme of one-channel gradiometer presented in Fig. 8 can be transformed into a multichannel scheme by adding the single-type sensors with the open feedback loop and using the self-oscillating sensor to support them. However, this procedure may actually allow only one line or column of a matrix because linear dimensions along the sensor axis are relatively large making a large distance between the matrix lines and columns.

Arranging the matrix positioning of sensors with a minimal gap would require to cancel optical elements before the photosensor and to substitute the latter by another sensor with an area of the photosensitive layer similar to absorbing cell bottom area. Given that design the cell bottom on the photosensor side could be brought to the object at a minimal

distance. The multitude of these edge sensors may cover the measurement field, i.e. the matrix.

The OPM gradiometer serves to measure the difference between the MF induction vectors while the SQUID or IM gradiometers are used to measure the difference between corresponding components of the induction vector module.

Assuming that the OPM sensor is affected by the geomagnetic field GMF *Bo* and also by the object's field ΔB at the θ angle to it, the measured field may be estimated as

$$Bobj = (B^2o + \Delta B^2 + 2\, Bo\Delta B \cos\theta)^{1/2}$$

If $\Delta B < Bo/10,000$ the approximated equation

$$Bobj = Bo + \Delta B \cos\theta$$

holds true with the 0.1% accuracy.

In case of a component device (SQUID, IM)

$$Bobj = Bo \cos\theta 1 + \Delta B \cos\theta 2,$$

where $\theta 1$ is the angle between the Earth's field direction and the projection axis, $\theta 2$ is the angle between the object's field direction and the projection axis. Thus, the OPM gradiometer can estimate the increment of MF from biological object in the GMF direction at the point of measurement by subtracting *Bo*. In order to measure the object's field components in different directions the object has to be turned against the direction of the GMF induction vector.

2.5. COMBINATION OF INDUCTION MAGNETOMETER AND SQUID

Combination of the different type magnetomers such as IM and SQUID to detect MF from a nerve impulse - spike is a special case [14].
As the nerve fiber size is quite small the magnitude of the SQUID detected MF is small as well. This is attributed to lack of correlation between the sizes of the SQUID MFT loop and the fiber. Besides, since the spike

duration (about I ms) is quite short the bandwidth of the magnetosensitive coil should be of the order of I kHz and more.

The nerve fiber and the SQUID magnetosensitive coil sizes are correlated by introducing an intermediate magnetosensitive induction coil wound on a small-size ferrite ring. There has been used a ferrite ring with magnetic permeability μ = 4000, external diameter - 3.4 mm, internal diameter - 1.2 mm, thickness - 1.1 mm. Number of wire turns on the ring - 35, diameter - 0.8 mm.

The induction coil is locked on the impedance-matching transformer made of a superconducting material such as the niobium wire with lead coating. The output winding of the transformer (NbTi wire) is locked on the SQUID through a coupling coil.

The impedance-matching transformer is placed in a helium bath together with the SQUID. To assure extra protection against the noise all superconducting SQUID elements and the impedance-matching transformer are held inside a cylindric superconducting screen. It should be noted that as the instrument is built according to the magnetometric design and is geared to respond to variations of the MF induction its noise immunity yersus gradiometers is relatively low. The instrument should be used together with an averaging unit fed from power supply and with a compensating circuit to adjust frequency characteristics of the magnetometer in the real time. All these steps allow to detect signal up to 10^{-7} A within the $1\text{-}10^{3}$ Hz frequency band without averaging. The averaging procedure may boost its current sensitivity to 40 nA/$Hz^{1/2}$.

2.6. HOW TO IMPROVE NOISE IMMUNITY IN MEASURING MF OF BIOLOGICAL OBJECTS

Today, measurement of MF of biological objects relies on three magnetometer types - IM, SQUID and OPM. Each type features its own intrinsic noise level. A low intrinsic noise level does not guarantee high resolution of the biological MF. The good resolution may be interfered

with high level natural GMF variations and the great deal of artificial noise frequently exceeding the natural variations level caused by anthropogenic activity in industrial areas. For instance, noise emitted by frequency networks in a lab or city hospital may exceed a biomagnetic field 1000-fold or more. Noise generated by electrified vehicles comes in pulses and reaches the order of dozens nT at a distance of hundreds of meters. Noise spectrum in towns practically overlaps the spectrum of signals from biological objects. As regards small towns and settlements and areas inside large city blocks they are dominated by natural GMF variations. Usually, the maximum GMF variation spectrum occurs within the large periods i.e, a day (30-50 nT depending on the town's geomagnetic latitude). It drops sharply in the short periods (50-100 pT, 1 s period) [41, 73]. The spectrum of geomagnetic variations usually expands into the short periods during strong magnetic storms which occur in the middle latitudes rather infrequently, and during magnetic disturbances typical of the high latitudes. Even the natural MF variations pose a serious obstacle to the biomagnetic research. Sometimes these hazards make it impossible to detect MF of biological objects in the background of the natural variations and even more so under the artificial noise.

There may be used a variety of different methods to control magnetic interference involving the use of differential measurement circuits, magnetic shields and coil systems. Differential measurement circuits should be rather used when the distance to the source of interference is at least hundred times larger than the distance between coils. The efficiency of differential measurement circuits will be described later. There should be carried out preliminary measurement of magnetic noise in the point of measurement. Also, there should be studied the MF topology and observed the magnetic hygiene rules prohibiting storage of ferromagnetic materials, instruments, electric motors and machines in or around the place designated for the subsequent installation of magnetosensitive sensors. It should be also remembered that shifting a magnetosensitive sensor in space during the measurement under the inhomogeneous MF would cause extra magnetic

interference.

Differential connection of the magnetometer sensors is one of the techniques to control magnetic interference from distant sources. Let us consider an alternative differential connection of two coils. It may be assumed that the transformation ratios of the both coils are identical. If the distance *r* between the coils (base distance) is considerably smaller than the distance *R* between the interference source located on the same line with the coil axes, which appears to be the most unfavorable mode of the noise location described by a certain magnetic moment *M*, the difference of the MF noise response of the two coils may be represented as

$$\Delta B = 3\ Mr/R^4.$$

Noise reduction in the differential regime versus magneto-metric connection will be

$$\beta = R/3r = l/3\alpha,$$

i.e. in proportion to the ratio between the noise source - sensors distance and the base.

It would appear that given a stationary object, noise reduction could be improved by reducing the distance between the coils. This, however, may cut down the valid signal level from the object positioned close to one of the sensors owing to the shift from the differential to gradient measurement when neglection of a small biomagnetic field detectable in the remote sensor volume is not allowed.

According to estimates, with $R \gg r$ the second-derivative gradiometer MF interference may be calculated as

$$\Delta B1 = 12\ Mr^2/R^5,$$

effective for the dipole interference source approximation.

Consequently, noise reduction of the second-derivative gradiometer versus the first-derivative gradiometer will be

$$\beta 1 = \Delta B/\Delta B1 = l/4\alpha.$$

As a increases the effectiveness of noise reduction in the second-derivative

gradiometer falls. At a certain a value it may fall to the first-derivative gradiometer level. This may occur if $\beta 1 = 1$ which corresponds according to the approximated ΔB and $\Delta B1$ to a = 0.25. In reality, parameter α is the smaller the better approximation of the MF gradients calculations. With $\beta 1 = 1$ the more accurate reading of parameter a will be 0.125-i.e. relative effectiveness of noise reduction in the first- and second-derivative gradiometers becomes equal with $8r = R$. All this brings us to the conclusion on the need to withdraw the source of interference or the sensors from it because the gradiometer design cannot assure infinite noise reduction.

The differential design of the instrument becomes gradientometric versus the external magnetic noise if the coils base is substantially smaller i.e. hundred times more than the distance to the source. From the object's side the measurement scheme is not gradientometric if the distance between the coil and the object is minimal. It will be rather differential or variational depending on whether the MF of the object affects two or one sensors, and its magnitude is below the noise level in the other sensor's volume. Therefore, the term "gradiometer" is not quite appropriate for the biomagnetic field measurements.

As a rule, magnetic shields are used in the detection of MF of the brain. In their magnitude these MF surpass the noise level of even the most low-noise instrument as SQUID very little. That is why in addition to the magnetic shield the SQUID sensors are connected according to the differential mode. Presence of interferences in the course of various biomagnetic researches makes it necessary to use the signal and signal spectrum accumulating systems.

Magnetic shield is, in fact, a device providing sharp external field (constant and alternating) attenuation within the shield volume. During its operation the magnetic flow is caused to concentrate on the shield walls manufactured of the high magnetic permeability material [93, 148] and is prevented from penetrating the shield.

Attenuation of the internal constant field within a single

layer shield may be approximately presented as

$$Bint/Bext \approx D/a\mu,$$

where D is the shield diameter, a is the wall thickness and μ is magnetic permeability.

From the point of design preference should be given to making a multi-layer shield from the high permeable than a single-layer thick material. The total rate of the internal field attenuation will be the product of individual layer rates. Owing to the skin-effect the attenuation rate will increase with the frequency growth.

Magnetic shields are manufactured from the high magnetic permeability material such as permalloy (μ = I—$2 \cdot 10^5$) of I mm thickness. The manufacture of large-size shields meets with certain design problems. The prepared (annealed) permalloy does not stand any mechanical impact. Therefore, bending, riveting, etc. should be avoided in the course of the shield frame making. As a rule the frame is made of a plain aluminum sheet. Two mutually perpendicular sets of permalloy bands are superimposed on it and covered by another aluminum sheet. This "sandwich" is then bonded with aluminum rivets. So, the aluminum sheets bear the main load. Usually, there are not more than three permalloy layers. The aluminum sheets are also used to control the high frequency noise.

Several new materials are also used in building shielded rooms such as the amorphous permalloy manufactured by flash freezing of liquid alloy.

The advantage of the amorphous permalloy over the regular annealed sheet permalloy is that its magnetic properties (magnetic permeability) are less dependent on the mechanical load.

As the new material thickness is less than 50 mcm the shield with more layers will be lighter than the one made of the regular 1-1.5 mm thick permalloy.

The shield should be fixed on supports emerging from the general foundation and have no mechanical contact with the walls and ceiling. This may help to avoid deformation of the shield's sheets during its operation.

The screening effect of the shield is improved by "magnetic shaking" reducing the mechanical stress in the permalloy sheets. Magnetic shaking is performed by continuous remagnetization of the top layer at a fixed frequency. It is done with additional external rings wound on the shield and connected to the power network. The process elicits the noise at frequencies multiple of the "shaking" frequency which is later attenuated in a narrow-band filter in a magnetometer.

A shield with over 10 m^3 internal volume can hold the object on a nonmagnetic bed, sensors and a laboratory assistant. Simplified shield versions fail to produce the desired effect due to the growing MF inhomogeneity inside the shield and drop of the attenuation rate.

Superconducting shields featuring high attenuation rate may be classified into a special group. However, their "warm volume" wherein the biological object may be safely placed is relatively small. As the "warm volume" inside the shield is usually less than 10 l the scope of the biomagnetic research appears to be limited.

There is also a different approach to attenuation of the external field and noise. This approach uses the ring systems fed with current controlled by MF sensors performing the function of compensating the field and its variations. The actual selection of the noise control system is eventually done with regard to the building and operational costs.

2.7. ACTIVE MEANS OF NOISE REDUCTION

In view of the technical problems the fast operation and measurement range of practically all types of gradiometer pick-up coils are limited. Therefore, active protection of the coil cuts down the absolute noise level and improves its operation. Magnetic interference may be reduced within the pick-up coil volume in the absense of a shielded chamber by the technique of the negative processing of coupling. Any type of coil may be used to identify the noise signal, amplify it and feed to the coil system

and elicit the MF in the phase opposite to the MF of the noise signal [49].

The coil system dimensions are related to the homogeneity within it and the size of the object. Detection of the biomagnetic field of the man would require a coil system that can house a man inside it. The uniform field volume within the system would expand with the increase in its dimensions but this will cause the transformation ratio i.e. the MF evoked per unit of current in the same number of the winding turns, to fall.

The coil-based active noise reduction system may be quite simple in its design because the magnitude of the magnetic noise in relation to the MF is 10^{-4}-10^{-3}. Inhomogeneity of the MF evoked by the current in the system would be proportional to the magnitude of the negative feedback current. If the system is made of the Helmholtz coils i.e. a pair of identical circular coils separated by a distance measuring to the circular coil radius, the uniform field volume will be 10^{-3} of the volume created by the ring coils. Assurping that the pick-up coil volume is 1 dm^3 the system's volume should be at least 1000 dm^3 and the minimal radius R of the system could be calculated as

$$R = (\nu/\pi)^{1/3},$$

where ν is the coil system volume and should be at least 65 cm. The Helmholtz coils constant Chc describing the current transformation rate in the MF may be estimated with the approximated equation

$$C\text{hc} \cong 89\ W/R\ [\text{nT/mA}],$$

where W is the number of the winding turns, R is the coils radius in cm. For instance, with $W = 100$ turns and $R = 65$ cm the Chc will be $\cong 140$ nT/mA.

The volume of the uniform compensation field may be increased by using the coil systems of complex configuration involving more than two coils having different number of turns and diameters [4, 74]. From the point of design preference is given to the system of five rectangular coils with equal quadrant side size but different number of turns. In that case

the volume created by the system is cube-shaped.

Noise reduction in the course of the componential gradiometry is performed with the three mutually orthogonal coil systems. The pick-up coils used for the noise identification must be componential as well and located close to the center of the system. The gradiometer's pick-up coil should be located in its center. Shifting of the noise pick-up coil from the center of the system having a small uniform field volume may result only in partial noise compensation in the center and smaller than in the volume of the pick-up coil.

To suppress strong magnetic noise of over 100-1000 nT there may be used fluxgate sensors operated in the null-detector regime i.e. indication of the MF component increment over its mean value. This approach requires the addition of a compensation coil into the fluxgate sensor featuring a relative instability of the order of 10^{-5}. In this case the noise of the order of 1 nT may be effectively eliminated within the sensor's volume.

Combination of gradiometric and variational MF sensors is the optimal noise reduction technique using the signal proportional to the level of variations and MF noise to assure noise immune operation of the gradiometer. It requires the variational sensor to be incorporated into the gradiometer. This technique can be also applied with OPM sensors because, as a rule, one of the sensors is operated in the autooscillating regime and its signal can be demodulated to know the noise variations. Since the OPM sensors are of the module type the coil system axis is set along the GMF direction. In the USSR territory the angle between the MF induction vector and the Earth's surface, referred to as inclination, lies in the order of $\theta = 60\text{-}80°$ i.e. it is possible to set the axis of the coil system perpendicular to the Earth's surface at the risk of a relatively small loss in the transformation rate (14% at $\theta = 60°$).

The block-scheme of the second-derivative OPM gradiometer is presented in Fig. 9. It shows: *D3* - autooscillating type *Dl* and *D2* - resonance sensors-filters. Signals from *Dl* and *D3* are fed to the phase detector *PD1* and signal from *D2* and *D3* - to the phase detector *PD2* making a pair

of a first-order gradients. Subtraction of one gradiometer's signal from another performed by the subtraction device *SD* is, in fact, the procedure of the second-order gradient estimation. Channeling of the gradiometer pair output signal through switches *S1* and *S2* and the low frequency filters *LFF* to the rf coils of sensors *Dl* and *D2* assures compensation of the MF difference between *D1-D3* and *D2-D3* pairs and normal operation of the *Dl*, *D2* - resonance filters i.e. maximal steepness of the gradiometer's transformation curve.

The frequency detector coupled to the *D3* output identifies the MF variations and noise which are further channeled through the low frequency filter *LFF* and dc amplifier *DCA*. The MF variations and noise are attenuated in the *Dl*, *D2* and *D3* when feedback current is fed to the coil system to evoke the MF having a reverse direction to the MF variation of noise.

Transformation rate *S*fd of the frequency detector should be high enough to obtain the required attenuation rate *S*fd may be estimated from

$$S\text{fd} \cong \beta / C\text{hc},$$

where β is the attenuation rate. In the previous example with *C*hc where β = 100 the *S*fd will be 0.73 mA/nT. Assuming that the Helmholtz coils resistance is 500 Ohm *S*fd in terms of tension will be 0.365 V/nT.

As the transconductance of the detuned circuit frequency detectors or ratio detectors used to transform the frequency modulated signal from the autooscillating OPM sensor is low and their retuning into another frequency band without loosing the permanent transconductance level is technically difficult, their use is quite problematic. Our purpose is better suited by the autocorrelating type frequency detector presented at the block-scheme (Fig. 10). The output signal from the *S*3 (Fig.9) is fed to the multiplying device directly and via the analog delay line. Delay time τd must be considerably longer than the input oscillation period. The delay line output oscillation is shifted in phase in relation to the input oscillation depending on its frequency. This shift is a periodic function. The frequency values

corresponding to knee-points of the amplitude-frequency static characteristic are reproduced in I/τd Hz intervals. The static characteristic is close to the sawtooth configuration. The bandwidth ΔF of the autooscillating detector operating

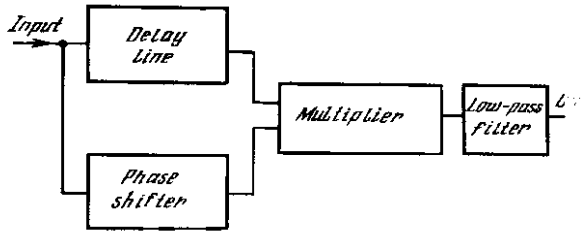

Fig. 10. Autocorrelating frequency detector

at a linear section of the statistical curve as

$$\Delta F = 0.45/\tau d.$$

If the detector's static characteristic meets the 1000 nT linear spread demand corresponding to the $\delta F = 3500$ Hz frequency variation in a cesium sensor, the required delay time /τd will be

$$\tau d = l/2\delta F = 66 \text{mcs}$$

and the bandwidth will be

$$\Delta F = 0.45/\tau d = 6750 \text{ Hz}.$$

Transconductance will be 0.005 V/nT at the multiplier's source voltage equal to 5 V. The further approximated calculation of the active noise control shows that attenuation rate $\beta = 100$ will require amplification factor of the order of 75. In case the sensor generated frequency coinsides with the knee-point on the detector's static characteristic an additional phase shift has to be made in one of the demodulator channels with phase shifter *FS* moving the working point into the middle of the static characteristic.

The autocorrelating detector design is related to the delay

line type. The use of the PK3-401 cable with 0.7 mcs/m delay prevents frequency transformation of the sensor signal. However, the required delay length with τd = 66 mcs will be 95 m which may be inappropriate in a particular design. It is possible to use a magnetostrictive delay line operated in the frequency range below I MHz. Application of the available ultrasonic color TV delay line of the UDL-64-2 or UDL-64-4 type with 64 mcs delay time necessitates introduction of a wide-band frequency multiplier before the detector because the UDL-64 operative frequency is 3-6 MHz while the generated frequency range controlled by the MF induction magnitude lies within the 75-300 kHz. In that case the required frequency multiplication rate will be 40 for the 75-150 kHz and 20 for the 150-300 kHz subranges. Dividing the direct and delayed signals frequency by the factor of 10 in the first and by the factor of 5 in the second subrange will produce a 1000 nT linear characteristic of the autocorrelating detector.

It is also possible to build the MF stabilizing system based on a OPM sensor and SQUID gradiometer coil. This alternative requires maximal spatial proximity of the two sensors and the gradiometer pick-up coil axis orientation along the GMF direction because stabilization is performed by the OPM sensors only in this direction.

2.8. ELIMINATION OF THE ELECTRIC NETWORK NOISE

Detection of the MF from biological objects is practically always hampered by the network noise coming from cable networks and electric appliances. Although the network noise level varies its frequency remains unchanged. The noise at the 50 Hz basic frequency features the highest amplitude. However, the spatial addition of the noise from various sources may elicit interference at higher harmonics or even at the 25 Hz subharmonic. Therefore, it is important to give adequate attention to the network noise elimination especially if a magnetosensitive coil is used in an unshielded room.

The noise difference signal is produced at the output of the gradiometric instruments used for magnetic measurements. Naturally, attenuation of the MF noise absolute level within the sensor volume will cause the noise signal to fall and the dynamic measurement range to expand. This process has been studied in paragraph 2.7, and here we are focusing on the alternatives. The first and most obvious alternative is to use a rejection filter to discriminate against the noise frequency in the signal amplification tract. There may be used a passive filter based on induction coils and capacitors or an active one based on resistors, capacitors and operational amplifiers. The network noise attenuation rate is related to the stability of parameters of the filter components and the network frequency stability. It is quite simple to make a passive filter with the attenuation rate of the order of 10-30. However, the passive filter rejection band is 3-10 Hz. Based on resistors, capacitors and modern operational amplifiers the active filters are capable of the network noise attenuation 50-100-fold at the rejection band less than 1 Hz.

The rejection factor may be increased by using several stages of the passive or active filters. Attenuation of the basic harmonic of the network noise does not increase the confidence, as it was earlier pointed out that the noise at other network harmonics remains low. In fact, one has to incorporate a set of filters tuned to discriminate at least against the first three network harmonics.

The other attenuation alternative is to single out the network noise and to feed it in the opposite phase to one of the gradiometer's sensors. The use of selector device under the high negative feedback causes the rises in the amplitude-frequency characteristic, falling on the slope of the selector device bandwidth. As they lead to the valid signal deterioration the feedback magnitude should be kept low. The third alternative is based on synchronous digitally controlled filters sometimes referred to as comb filters [71]. Since operation of the filter is synchronized with the network frequency and its harmonics the filter is capable to follow all variations of the network frequency.

A simple filter scheme is presented in Fig.11. The summary charge in the capacitors is close to zero if the input signal frequency does not match the frequency of commutation. When the frequencies are equal the output voltage of amplifier *V* reaches its maximum and the current

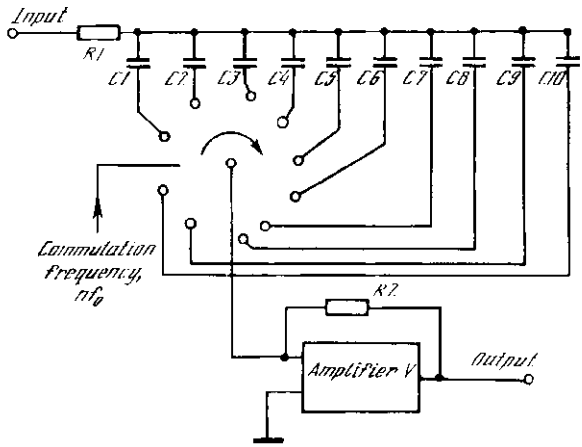

Fig. 11. Digitally controlled filter for the network noise attenuation

in the commutator drops to minimum. The operational amplifier *V* is used to transform *i*out into voltage. The same process occurs with the multiple ratio of the frequencies. The filter's resonance frequence is related to the commutation frequency, the rejection band - to the *nRC* time constant, where *n* is the number of commuted capacitors. With $\tau = RC = 0.2$s and number of capacitors $n = 32$ the comb filter can attenuate the first network harmonic by 40-45 dB and other harmonics in a smaller degree in the 0.1 Hz rejection band. Cascading of two comb filters may improve the first harmonic attenuation to over 80 dB. The filter's dynamic range is related to the admissible voltage at the electronic keys responsible for the commutation. The key operation time is $1/nT$, where *T* is the commutation period, *n* - number of keys.

2.9. ON THE APPROPRIATE BANDWIDTH OF THE MAGNETOMETRIC DEVICES

The spectrum of frequencies involved in the measurement of MF of biological objects is quite wide. For example, in the course of taking an MCG the signal frequencies spectrum is basically related to the wave form *QRS*. It has been found that a cardiogram recorded with 30 harmonics of the basic frequency i.e. frequency of the cardiac rhythm actually reproduces 97% of the total information. Relying on this criterion the minimal bandwidth is estimated at 30-40 Hz. The lower boundary of the bandwidth is related to the cardiogram wave distortion. In order to keep distortion at minimum the lower frequency is usually set at the one order less than the cardiac rhythm i.e. the lower boundary of the bandwidth is within 0.07 = 0.1 Hz.

Velocity of the frequency characteristic fall outside the bandwidth must not be large. Otherwise, after the *QRS* complex ending the MCG will show an attenuating oscillation evoked by the transition in the signal amplification tract.

Devices with the limited bandwidth reproduce the wave similar to the *QRS* complex most reliably if attenuation outside the bandwidth is filtered in low frequency Bessel filters to assure uniform delay phase to all harmonics of the *QRS* complex.

Detection of the evoked (usually by the applied MF) magnetization in the tissue, blood or bone formations usually produces the signal close to 0 Hz. As regards the uppci boundary it is related to the velocity of the approaching or moving apart coil and the object.

Taking of a magnetomiogram involves shifts of the bandwidth into the high frequency area with the lower boundary to the order of several Hz and the upper boundary to the order of several hundred Hz.

The magnetooculographic devices usually operate in a narrow bandwidth. The central bandwidth frequency is related to the eye lid movement frequency. The MEG signal range is quite wide. It may range from

the frequencies of the order of several Hz to the order of several dozen Hz. Taking a MEG involves division of the total bandwidth into several bands with the view to improve the signal-to-noise characteristic. For example, detection of the alpha-rhythm of the human brain is performed in the 3-5 to 25-30 Hz ranges.

Detection of MF evoked in the brain by various stimuli such as light, sound, etc. is a special case. As a rule there are applied short strong random stimuli. Duration of the brain response appears to be longer than the stimulus itself. The brain response is usually recorded during 0.5 s at maximum. The bandwidth corresponding to this duration is relatively small because no dramatic signal wave distortion is observed during the response.

Detection of the MF of a nerve impulse (spike) having a very short duration requires at least a 1 kHz bandwidth. Owing to the low signal-to-noise ratio the evoked MF can be detected, as a rule, with the use of synchronized accumulation facilities. The signal-to-noise ratio is proportional to the square root of the number of accumulations at the normal Gaussian noise.

2.10. RELATION OF THE SIZE OF MAGNETOSENSITIVE SENSOR TO THE RESULTS OF THE BIOMAGNETIC FIELD DETECTION

The magnetometric measuremem facilities show the maximal resolution (sensitivity) in detecting a uniform MF within the volume of any type sensor.

Sizes of the coil and the MF source become comparable when magnetometer has to deal with MF from biological objects or particularly when MCG or MEG is taken. The pattern of the MF inhomogeneity is related to the source type which may be described as an equivalent magnetic dipole, quadrupole or combination thereof. Consequently, the field from the biological object is not homogeneous within the pick-up coil volume. For instance, if the MF source is presented as a magnetic dipole of the size smaller than the pick-up coil the average MF magnitude within the OPM

gradiometer pick-up coil volume is three times smaller than the maximal field magnitude at the margin assuming that distance from the dipole to the pick-up coil measures to the pick-up coil diameter.

If IM or OPM are used the signal from the biological object is integrated by the volume of the pick-up coil sensitive element or by the loop area of the flux transformer in SQUID. Therefore, it is essential to take into account the difference between the obtained reading of the biomagnetic field and maximal magnitude.

The pick-up coil size reduction improves the spatial resolution and upgrades precision of the biomagnetic induction measurement. The side effect of this will be the fall of sensitivity. In SQUID the problem of matching the spatial resolution with the invariable sensitivity is resolved by the use of asymmetric pick-up coil in the first- and second-derivative gradiometers (Fig. 4,*f*,g). For other sensors it is necessary to find a compromise for the sizes and to use corrections.

2.11. MECHANICAL SUPPORTS USED IN THE BIOMAGNETIC RESEARCH

A module or a component type sensor should be rigidly fixed in space because its motion through a nonhomogeneous MF causes artefacts the magnitude of which can substantially surpass the valid signal from the biological object.

The Earth's permanent MF is quite homogeneous. Its mean gradient is about 5-10 pT/m. Magnetic masses such as radiators and pipes of the heating, ferroconcrete structures, elevator shafts and other steel objects eliciting their own MF and distorting the natural GMF topology are usually present around the room where the biomagnetic research is carried out. Other sources of the nonhomogeneous MF are electronic units, measuring instruments and plotters composing the magnetometric hardware. This fact makes placing them at a distance from the magneto-sensitive pick-up coil a must. It is quite problematic to estimate the expected magnitude of the MF and the noise level elicited by induction in the steel structures. Therefore, prior to the pick-up coil installation and the biomagnetic research

there should be estimated the MF gradient and its variations in the work room with the portable M-33, KM-2, KM-8 and other industrially manufactured instruments. Preliminary study allows to estimate the possibility of proceeding with the biomagnetic research in a given place or hints the appropriate steps to reduce the MF gradient and the noise level. The gradient compensation in a small range may be performed by permanent magnets placed at 2-3 m from the magnetosensitive coil. The magnet's position in space is selected in accordance with the MF gradient minimum in the sensor's volume.

The sensor must be fixed rigidly. Elements of its mounting should be made of nonmagnetic materials such as caprolactan, polypropylene, paper- and cloth-based laminates, duralumin. However, metal fittings with good conductance should not be located in the environs of the pick-up coil to prevent induction current in them. It is also undesirable to use the magnesium-aluminum alloy because photoelectric currents are elicited in it by light.

The magnetosensitive coil may be fixed on a mount having no mechanical contact with the object's bed, or on a wall or ceiling mounting.

Beneath the sensor there is a horizontal platform movable along the two rectangular coordinates where the object is placed in the lying position. The platform motion along the two coordinates allows to place the appropriate part of the object within the sensor's range. It is also desirable to provide a hoistering-lowering mechanism facilitating measurement in accordance with configuration of the object's body. Besides, the platform should have the minimum number of the nonmagnetic metal parts. The mat and pillow on the platform should be comfortable enough for the object as some biomagnetic measurements may be quite long and last dozens of minutes. Various types of mechanical supports used in taking magnetograms of the man are briefly presented in the publication [84], lung inclusions in [45], evoked MF of the human brain in [14, 50].

2.12. MEASUREMENT OF MAGNETIC SUSCEPTIBILITY OF THE BIOLOGICAL OBJECTS

The measurement of magnetic susceptibility of the biological objects amounts to measuring the additional MF elicited in the object by the impact of MF, owing to its dia- and paramagnetic properties. What is usually required is the susceptibility of individual parts of the biological object rather than of the whole object.

Magnetic susceptibility is measured with a device made of two coils wound of a superconducting material. One coil is geared to induce the magnetizing field Br and the other to receive the field variations. According to the estimates the maximal signal may be obtained by placing the coils as close as possible to each other, and the contribution from a particular part of the body may be identified by having a uniform and parallel field within the designated volume and weak and nonparallel in other parts. The measurement of magnetic susceptibility is interfered with by irregular form of the object and inhomogeneity of its magnetic susceptibility.

Speaking in practical terms this technique amounts to evoking a MF induction of the order of 10 mT with a superconducting coil placed close to the pick-up coil. Stability of the field of the superconducting coil is assured by its short-circuiting. Susceptibility measurement was conducted in a shielded room [146]. This method was instrumental in measuring the human cardiac blood volume with the view to estimate the blood flow intensity.

A similar method has been used to measure magnetic susceptibility of excessive iron in the liver [45]. In this case it was necessary to move the object to and from the pick-up coil in order to perform the differential measurement. The impact of the surface skin layers to which the coil is more sensitive was neutralized by an elastic rubber balloon with water under permanent pressure placed between the body and the SQUID gradiometer dewar. This method made it possible to neglect configurations of the body and to regard the liver as an object with flat surface and unlimited depth. The resolution was high enough to estimate the iron concentration with the

precision corresponding to the normal magnetic liver susceptibility.

The error of this technique is related to the accuracy of the ultrasonic measurement of the distance between the object's surface and the proximal liver surface.

The technique may be improved by eliciting the magnetizing field with Helmholts coils at the room temperature. The method can hardly evoke a more than 0.1 mT field, larger fields would require considerable energy input. This magnitude appears to be insufficient for the dc measurements with the noise having the maximum frequency spectrum at frequencies close to zero. The ac method has been applied to shift the operative band from the environs of zero to the area above 10 Hz where the noise level falls dramatically [148]. It involved feeding the magnetizing coil with ac and detection of the signal with the second-derivative SQUID gradiometer. Its output signal was locked on the synchronous detector. This approach may be quite helpful in assaying the characteristics of large or irrefular objects or in quick estimating of several samples which merely have to be brought and removed from the SQUID's dewar.

It should be noted that the result of the human MF measurement against the MGF background incorporates the part provided by the object's magnetic susceptibility. The contribution of the component of the osseous skeleton particularly in the thorax and joints is especially impressive. The impact of the object's magnetic susceptibility may be eliminated or reduced, for example, in the MCG by limiting the bandwidth of the measuring tract in the realm of low frequencies. The other alternative is to work in the zero MF.